

ANL/CHM/CP-98229

Forward-Backward Asymmetries of Atomic Photoelectrons

S. H. Southworth, B. Krässig, E. P. Kanter, J. C. Bilheux,
R. W. Dunford, D. S. Gemmell, S. Hasegawa, and L. Young

Argonne National Laboratory
Argonne, Illinois 60439, USA
e-mail: southworth@anl.gov

RECEIVED
OCT 13 1998
O.S.T.I.

Abstract

When atomic photoionization is treated beyond the dipole approximation, photoelectron angular distributions are asymmetric forward and backward with respect to the direction of the photon beam. We have measured forward-backward asymmetries of Ar 1s and Kr 1s and 2s photoelectrons using 2-19 keV x-rays. The measured asymmetries compare well with calculations which include interference between electric-dipole and electric-quadrupole amplitudes within the nonrelativistic, independent-particle approximations.

Theoretical concepts

Consider photoionization of randomly-oriented atoms by a linearly-polarized, narrow-band photon beam from a synchrotron radiation beamline. In nonrelativistic, first-order perturbation theory, the transition matrix element between initial and final electron states $|i\rangle$ and $|f\rangle$ can be expressed as

$$M_{if} = \langle f | \exp(i\mathbf{k} \cdot \mathbf{r}) \mathbf{e} \cdot \mathbf{p} | i \rangle, \quad (1)$$

where \mathbf{k} is the photon propagation vector, \mathbf{r} is the electron position vector, \mathbf{e} is the photon polarization vector, and \mathbf{p} is the electron momentum vector [1,2]. Referring to Fig. 1, the orthogonal vectors \mathbf{e} and \mathbf{k} define a rectangular coordinate system with which to measure photoelectron angular distributions. In general, angular distributions will depend on the angles between the photoelectron momentum \mathbf{p} and both \mathbf{e} and \mathbf{k} . We assume here that the photon beam is completely linearly polarized and choose the polar angle θ to be measured from \mathbf{e} to \mathbf{p} , and the azimuthal angle ϕ is measured from \mathbf{k} to the projection of \mathbf{p} in the plane perpendicular to \mathbf{e} .

The submitted manuscript has been created by the University of Chicago as Operator of Argonne National Laboratory ("Argonne") under Contract No. W-31-109-ENG-38 with the U.S. Department of Energy. The U.S. Government retains for itself, and others acting on its behalf, a paid-up, nonexclusive, irrevocable worldwide license in said article to reproduce, prepare derivative works, distribute copies to the public, and perform publicly and display publicly, by or on behalf of the Government.

DISCLAIMER

This report was prepared as an account of work sponsored by an agency of the United States Government. Neither the United States Government nor any agency thereof, nor any of their employees, make any warranty, express or implied, or assumes any legal liability or responsibility for the accuracy, completeness, or usefulness of any information, apparatus, product, or process disclosed, or represents that its use would not infringe privately owned rights. Reference herein to any specific commercial product, process, or service by trade name, trademark, manufacturer, or otherwise does not necessarily constitute or imply its endorsement, recommendation, or favoring by the United States Government or any agency thereof. The views and opinions of authors expressed herein do not necessarily state or reflect those of the United States Government or any agency thereof.

DISCLAIMER

**Portions of this document may be illegible
in electronic image products. Images are
produced from the best available original
document.**

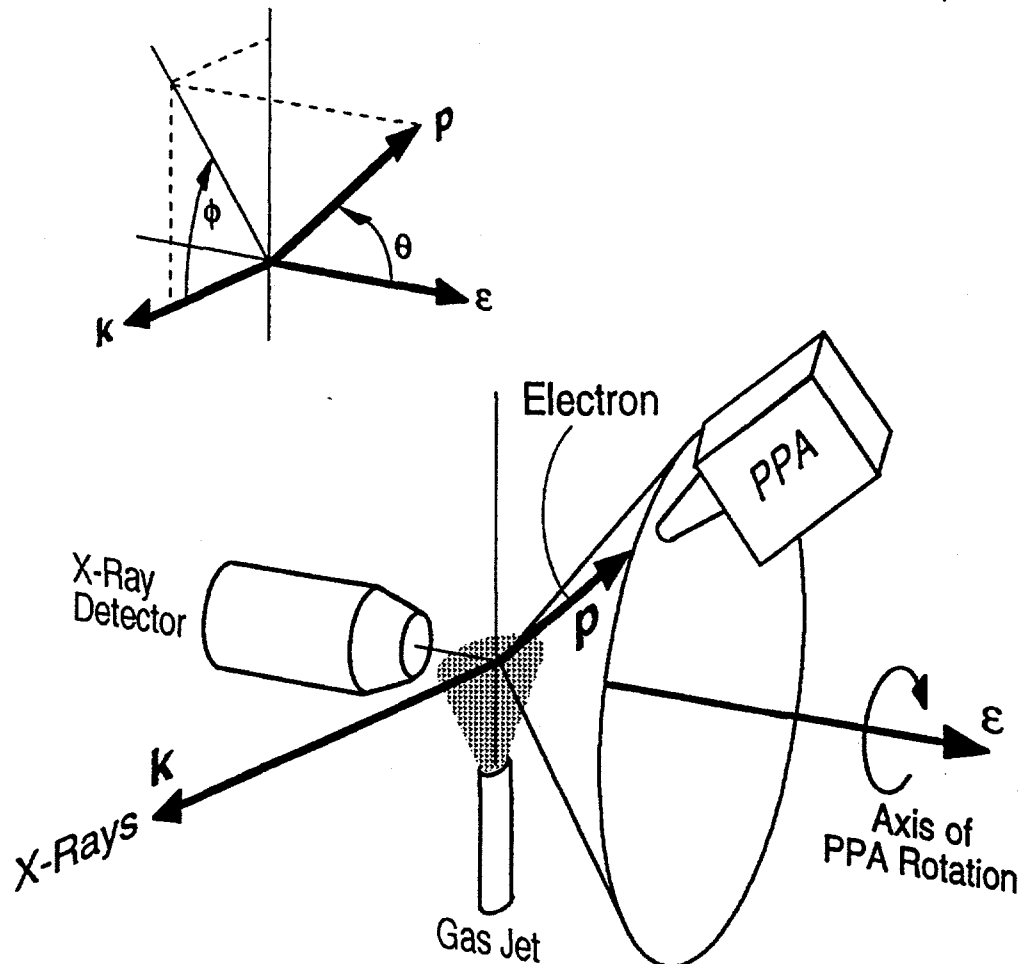


FIG. 1. Schematic diagram of the experimental system used for measurements of forward-backward photoelectron asymmetries. The PPA is a parallel-plate electron energy analyzer. The photoelectron momentum \mathbf{p} is measured relative to the polarization vector $\mathbf{\epsilon}$ and propagation vector \mathbf{k} of the x-ray beam.

If $\mathbf{k} \cdot \mathbf{r} < 1$, the exponential factor in Eq. (1) can be expanded as

$$\exp(i\mathbf{k} \cdot \mathbf{r}) \approx 1 + i\mathbf{k} \cdot \mathbf{r} - (1/2)(\mathbf{k} \cdot \mathbf{r})^2 + \dots \quad (2)$$

And if the photon wavelength $\lambda = 2\pi/k$ is large compared with the radius r of the initial electron state, the series (2) is often truncated at the leading term

$$\exp(i\mathbf{k} \cdot \mathbf{r}) \approx 1, \quad (3)$$

and the matrix element becomes

$$M_{if} \approx \langle f | \mathbf{e} \cdot \mathbf{p} | i \rangle. \quad (4)$$

In connection with a multipole expansion of the photon-electron interaction [3], Eqs. (3) and (4) correspond to pure electric-dipole (E1) interaction in the long-wavelength limit ($k \rightarrow 0$). The E1 approximation results in well-known selection rules on allowed changes in angular momentum and parity and restricts the form of the differential cross section to

$$d\sigma/d\Omega = (\sigma/4\pi)[1 + (\beta/2)(3\cos^2\theta - 1)], \quad (5)$$

where σ is the angle-integrated cross section and β is the photoelectron anisotropy parameter. Synchrotron radiation has been used extensively to study variations of the dynamical parameters σ and β with photon energy [4]. In the E1 approximation, the photoelectron angular distribution is completely characterized by the β parameter and is symmetric with respect to reversal of the direction of the photon beam, i.e., there is no forward-backward asymmetry.

If the second term in the expansion (2) is included,

$$\exp(ik \cdot r) \approx 1 + ik \cdot r, \quad (6)$$

then the transition matrix element

$$M_{if} \approx \langle f | (1 + ik \cdot r)(\epsilon \cdot p) | i \rangle \quad (7)$$

includes the long-wavelength limits of electric-dipole (E1), electric-quadrupole (E2), and magnetic-dipole (M1) interactions [1-3]. Bechler and Pratt [1] and Cooper [2] have made photoionization calculations for various atomic subshells based on Eqs. (6) and (7) using the nonrelativistic, independent-particle approximations (NR-IPA). In those calculations, made for photoelectron kinetic energies from threshold to several keV, the M1 amplitudes vanish and the pure E2 contributions to the angle-integrated cross section σ are negligible in comparison with the dominant E1 contributions. The key result is to explain how interference between E1 and E2 amplitudes redistributes photoelectron intensity forward and backward with respect to the photon beam. Using Cooper's [2] notation, the differential cross section is expressed

$$d\sigma/d\Omega = (\sigma/4\pi)[1 + (\beta/2)(3\cos^2\theta - 1) + (\delta + \gamma\cos^2\theta)\sin\theta\cos\phi], \quad (8)$$

where σ and β are the same as in Eq. (5) and the parameters δ and γ characterize the forward-backward asymmetry. The angular factors in Eq. (8) are related to vector dot products: $\cos\theta = \hat{\epsilon} \cdot \hat{p}$ and $\sin\theta\cos\phi = \hat{p} \cdot \hat{k}$. The angular factor $\hat{p} \cdot \hat{k}$ ranges from 1 for p parallel to k , to 0 for p perpendicular to k , to -1 for p antiparallel to k , and its integral over all angles is 0, so the terms involving δ and γ simply redistribute photoelectron intensity. The form of Eq. (8) is

symmetric with respect to reflection in the planes parallel and perpendicular to ϵ but is asymmetric with respect to reflection in the plane perpendicular to \mathbf{k} .

If the dipole approximation (Eq. (5)) is assumed to be valid and measurements are made in the forward or backward directions, determinations of σ and β will be in error in cases for which the δ and γ terms are significant. However, the δ and γ terms do not affect measurements made in the plane perpendicular to \mathbf{k} , because Eq. (8) reduces to Eq. (5) in that plane. But is Eq. (8) a sufficient description of the angular distribution? Is it necessary to include the next term in Eq. (2), which introduces electric-octupole (E3) amplitudes? LaJohn and Pratt [5] have made theoretical studies of this question, and it is being investigated in Kr 1s asymmetries recently measured using 14-19 keV x-rays [6]. Our earlier measurements for Ar 1s and Kr 2s and 2p using 2-5 keV x-rays [7] agree well with NR-IPA calculations [1,2] based on Eqs. (7) and (8), and we will assume those approximations to be valid in the discussion here. Equation (8) has also been used to interpret forward-backward asymmetries for Ne 2s and 2p using 250-1200 eV soft x-rays [8], for autoionizing levels of Cd near 13 eV [9], and for photoemission from surface-adsorbed atoms in x-ray standing wave experiments [10].

In the NR-IPA, the theoretical description of the photoionization of atomic s-subshells is relatively simple and gives insight into the physics of photoelectron asymmetries [1,2]. The E1 interaction produces a p-wave ($ns \rightarrow \epsilon p$) and $\beta = 2$. The E2 interaction produces a d-wave ($ns \rightarrow \epsilon d$) which interferes with the p-wave. However, $\delta = 0$, and the forward-backward asymmetry is described by the γ parameter alone. Putting $\beta = 2$ and $\delta = 0$ into Eq. (8) gives

$$d\sigma/d\Omega = (3\sigma/4\pi)\cos^2\theta[1 + (\gamma/3)\sin\theta\cos\phi]. \quad (9)$$

The $\cos^2\theta$ distribution of a pure $ns \rightarrow \epsilon p$ transition is modified by the $(\gamma/3)\sin\theta\cos\phi$ interference term. The dynamical parameter γ can be expressed as

$$\gamma = 3k(Q_2/D_1)\cos(\delta_2 - \delta_1), \quad (10)$$

where D_1 and δ_1 are the dipole matrix element and phase shift, respectively, for the $ns \rightarrow \epsilon p$ transition, and Q_2 and δ_2 are the quadrupole matrix element and phase shift, respectively, for the $ns \rightarrow \epsilon d$ transition. Equation (10) shows that $|\gamma|$ increases with increasing photon energy $E = \hbar\omega k$ and increases when Q_2 is relatively large or D_1 is relatively small. Bechler and Pratt [1] have also shown for 1s-subshells that negative values of γ can be traced to the phase shift difference $\delta_2 - \delta_1$.

Experimental methods

Shaw *et al.* [11] have discussed various experimental approaches to measurements of β , δ , and γ and considered effects of partial polarization and angular misalignment. The experimental system we have developed is shown in Fig. 1, and the measurement methods and data analysis procedures have been discussed in detail [7]. We use a parallel-plate electron analyzer (PPA) which is rotatable around the ϵ axis at fixed polar angle $\theta = \cos^{-1}(3^{-1/2}) \approx 54.7^\circ$. This is the magic angle which eliminates terms involving β from Eqs. (5) and (8) in the limit of a 100% linearly-polarized photon beam. Putting $\cos^2\theta = 1/3$ and $\sin\theta = (2/3)^{1/2}$ in Eq. (9) for atomic s-subshells gives

$$d\sigma/d\Omega = (\sigma/4\pi)[1 + (2/27)^{1/2}\gamma\cos\phi]. \quad (11)$$

The γ parameter is determined from photoelectron intensities measured with the PPA positioned at a set of angles ϕ . For our first experiments [7], measurements were made over the range $\phi = 0^\circ - 360^\circ$ in 15° steps in order to confirm the functional form of Eq. (11). It is necessary to account for an instrumental asymmetry due to variation with angle of the portion of the source volume collected by the PPA and perhaps due to misalignment or external fields. The spectrometer is shielded from the earth's magnetic field with mu-metal, and the PPA and its rotation axis are carefully aligned with the gas jet and photon beam to minimize such effects. The remaining instrumental asymmetry is determined by measurements of Auger electrons, which have no forward-backward asymmetries in the limit of a two-step process [12]. It is also necessary to account for deviations from 100% linear polarization and for misalignment of the PPA rotation axis with the polarization ellipse. These effects are essentially eliminated by averaging photoelectron intensities made in the upper half-plane ($0^\circ - 180^\circ$) with those in the lower half-plane ($180^\circ - 360^\circ$) [7].

The rotatable PPA system was recently used to measure forward-backward asymmetries of Kr 1s photoelectrons at Argonne's Advanced Photon Source [6]. An electron spectrum recorded at an x-ray energy of 14.826 keV, which is 500 eV above the Kr 1s ionization energy, is shown in Fig. 2. Along with the Kr 1s photopeak in Fig. 2 are low-energy and high-energy Auger transitions which were used to determine the instrumental asymmetry. To account for variations in x-ray beam intensity and sample gas density, the electron intensities measured at

each angle are normalized with respect to the intensities of scattered and fluorescent x-rays recorded by an x-ray detector positioned opposite the PPA (see Fig. 1).

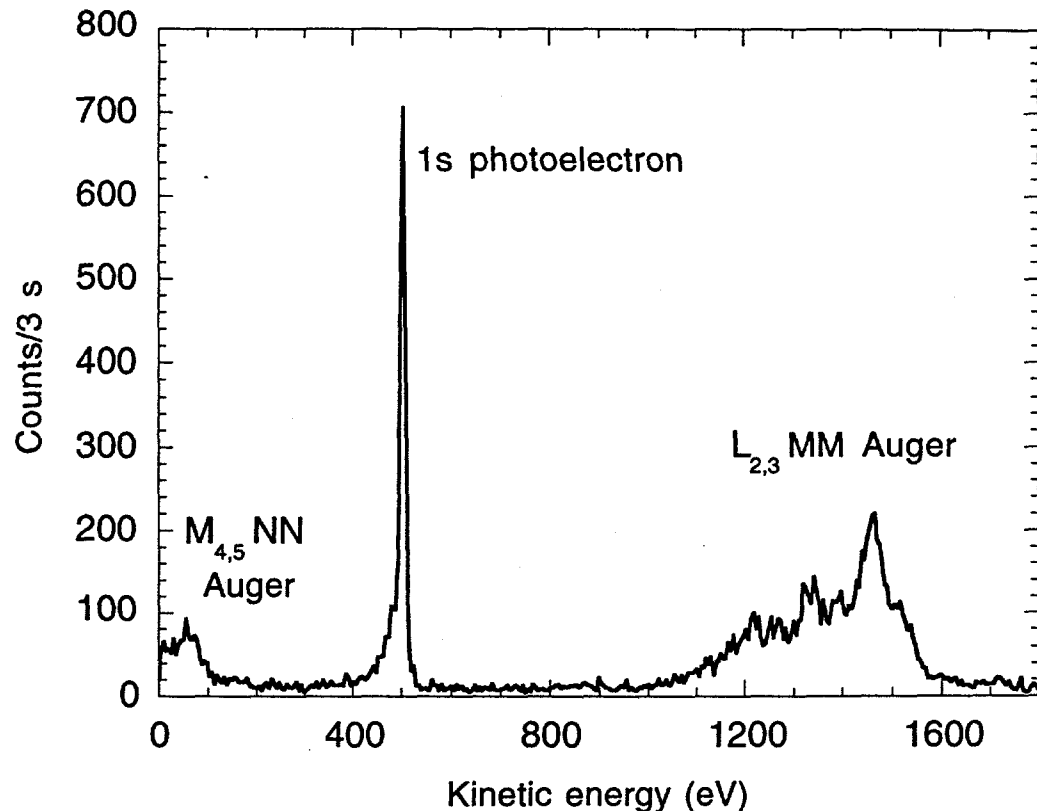


FIG. 2. Kr 1s photoelectron and Auger electron spectrum recorded 500 eV above threshold.

Based on data analysis methods developed for our first experiments [7] and general considerations of the dependence of angular distributions on photon beam polarization [13], we determined γ parameters from electron intensities at only four angles, $\phi = 45^\circ, 135^\circ, 225^\circ$, and 315° . These angles are "magic" with respect to both ϵ and \mathbf{k} , and the intensities are independent of the degree of polarization [7,11,13]. To account for small misalignments of the PPA rotation axis with the polarization ellipse [7], the forward intensity is taken as the average of the 45° and 315° measurements, and the backward intensity is taken as the average of the 135° and 225° measurements.

Results

The relative intensities of Kr 1s photoelectrons measured at the four angles for three x-ray energies and for Kr L_{2,3}MM Auger electrons are plotted in Fig. 3.

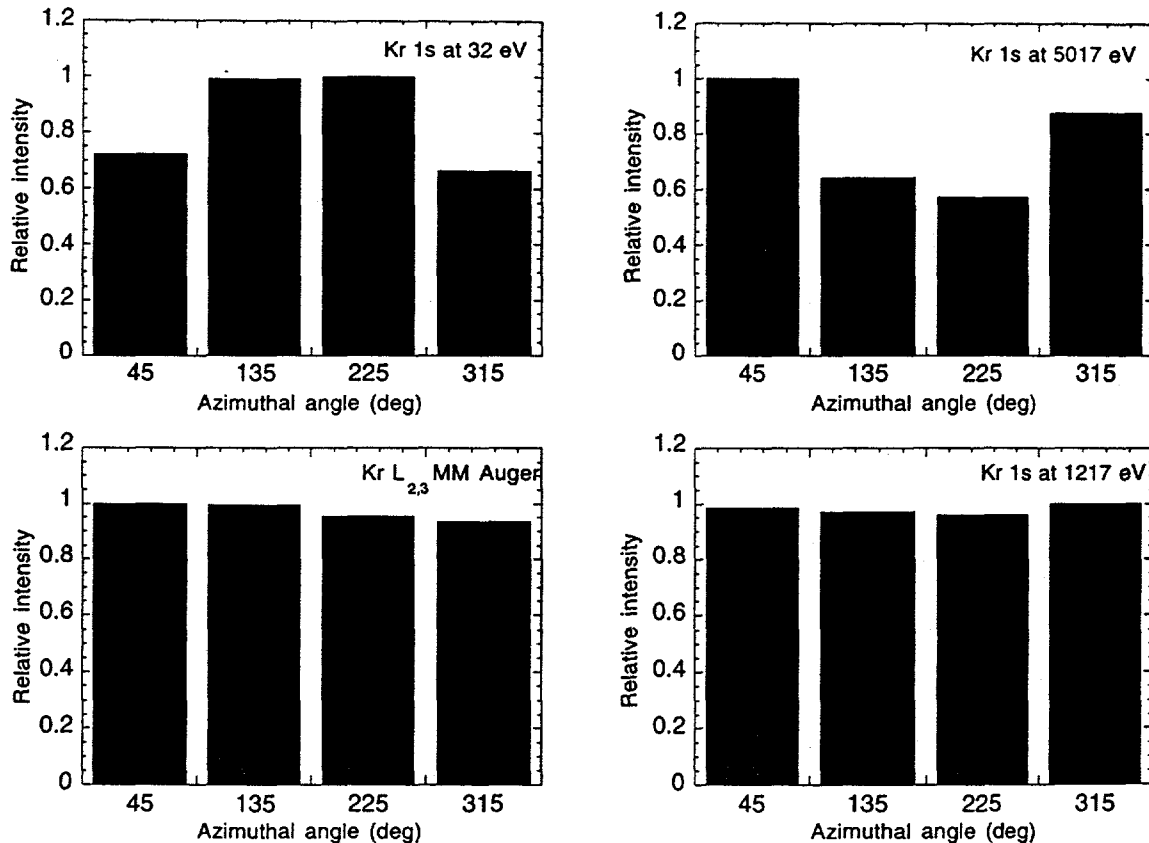


FIG. 3. Angular dependence of the relative intensities of Kr 1s photoelectrons measured at 32 eV, 1217 eV, and 5017 eV above threshold and for Kr L_{2,3}MM Auger electrons.

The Auger electron intensities should be isotropic, but show a small up-down instrumental asymmetry which is accounted for in deriving γ values from the photoelectron intensities. The Kr 1s intensities at 32 eV above threshold are larger at 135° and 225° (backward) than at 45° and 315° (forward), indicating $\gamma < 0$. At 1217 eV above threshold, the Kr 1s intensities are nearly the same, indicating $\gamma \approx 0$. And at 5017 eV above threshold, the forward intensities are

larger than the backward intensities, indicating $\gamma > 0$. These results are consistent with the asymmetries calculated for Kr 1s by Bechler and Pratt [1] using NR-IPA wavefunctions. We made measurements of Kr 1s asymmetries for several kinetic energies between threshold and 5 keV [6]. However, final results for γ parameters have not yet been determined for inclusion in this report.

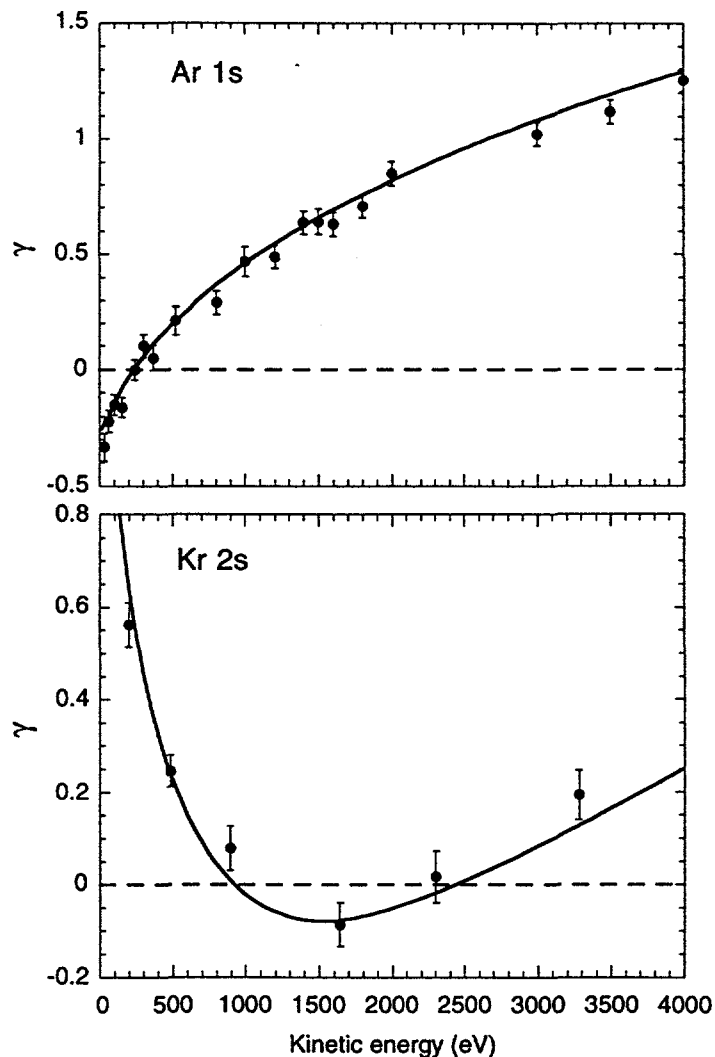


FIG. 4. Forward-backward asymmetry parameters γ calculated [1,2] and measured [7] for Ar 1s and Kr 2s photoelectrons vs. kinetic energy.

We conclude with a comparison in Fig. 4 of γ parameters calculated [1,2] and measured [7] for Ar 1s and Kr 2s for kinetic energies from approximately threshold to 4 keV. The γ

parameters for the two subshells show very different variations with energy. The Ar 1s asymmetry is negative near threshold, passes through zero, and becomes increasingly positive (forward directed) with increasing energy. The Kr 2s asymmetry is positive near threshold, drops through zero to become slightly negative, then passes through zero again and becomes increasingly positive at high energy. The differences in γ parameters for the two s-subshells can be traced to the theoretical factors in Eq. 10 [1]. For Ar 1s, Q_2 and D_1 remain positive, and the negative γ values near threshold are due to the phase-shift factor $\cos(\delta_2 - \delta_1)$. For Kr 2s, the node in the initial-state radial function causes Q_2 to be negative near threshold before changing to positive at higher kinetic energies and results in the double-zero in γ . Connections between forward-backward asymmetries and theoretical concepts provide insight into photoionization processes similar to those from experimental and theoretical studies of σ and β [4]. Not shown in Fig. 4 are additional oscillations in γ predicted below ≈ 20 eV [1]. Low-energy electron spectroscopy has both practical and physical complications, particularly in the x-ray regime, but we have looked for this threshold effect in our Kr 1s measurements and will report on it elsewhere [6].

Acknowledgements

We thank the staff at the Basic Energy Sciences Synchrotron Radiation Center at the Advanced Photon Source for support in conducting experiments. We thank L. A. LaJohn and R. H. Pratt for discussions of theory and providing calculated results. This work was supported by the U. S. Department of Energy, Office of Basic Energy Sciences under Contract No. W-31-109-ENG-38.

References

- [1] A. Bechler and R. H. Pratt, *Phys. Rev. A* **39**, 1774 (1989) and *Phys. Rev. A* **42**, 6400 (1990).
- [2] J. W. Cooper, *Phys. Rev. A* **47**, 1841 (1993).
- [3] M. Peshkin, *Adv. Chem. Phys.* **18**, 1 (1970).
- [4] See, for example, V. Schmidt, *Rep. Prog. Phys.* **55**, 1483 (1992).
- [5] L. A. LaJohn and R. H. Pratt, *Phys. Rev. A* **58**, 4989 (1998).

- [6] S. H. Southworth, B. Krässig, E. P. Kanter, J. C. Bilheux, R. W. Dunford, D. S. Gemmell, S. Hasegawa, and L. Young, unpublished.
- [7] B. Krässig, M. Jung, D. S. Gemmell, E. P. Kanter, T. LeBrun, S. H. Southworth, and L. Young, *Phys. Rev. Lett.* **75**, 4736 (1995) and *Phys. Rev. A* **54**, 2127 (1996).
- [8] O. Hemmers, G. Fisher, P. Glans, D. L. Hansen, H. Wang, S. B. Whitfield, R. Wehlitz, J. C. Levin, I. A. Sellin, R. C. C. Perera, E. W. B. Dias, H. S. Chakraborty, P. C. Deshmukh, S. T. Manson, and D. W. Lindle, *J. Phys. B* **30**, L727 (1997).
- [9] N. L. S. Martin, D. B. Thompson, R. P. Bauman, C. D. Caldwell, M. O. Krause, S. P. Frigo, and M. Wilson, *Phys. Rev. Lett.* **81**, 1199 (1998).
- [10] C. J. Fisher, R. Ithün, R. G. Jones, G. J. Jackson, D. P. Woodruff, and B. C. C. Cowie, *J. Phys.: Condens. Matter* **10**, L623 (1998).
- [11] P. S. Shaw, U. Arp, and S. H. Southworth, *Phys. Rev. A* **54**, 1463 (1996).
- [12] N. M. Kabachnik and I. P. Sazhina, *J. Phys. B* **29**, L515 (1996).
- [13] M. Peshkin, in "Atomic Physics with Hard X-Rays from High Brilliance Synchrotron Light Sources," Proceedings of a Workshop held at Argonne National Laboratory, May 20-21, 1996, report no. ANL/APS/TM-16, p. 207.